A Lumped Specific Heat Capacity Approach for Predicting the Non-stationary Thermal Profile of Coffee During Roasting

M. Basile and I. Kikic*

Department of Chemical, Environmental and Raw Materials
Engineering (DICAMP), University of Trieste,
Piazzale Europa 1, 34127 Trieste – Italy

Coffee undergoes numerous and relevant chemical and physical changes during roasting. These modifications lead to the development of those typical organoleptic properties of coffee, on which the acceptability of the product depends. The roasting process therefore, plays a central role within the coffee's technological cycle. This crucial character of roasting has contributed to encouraging the continuous progress of the roasting industry incorporating the necessary scientific and technological research.

However, due to the geometrical complexity and transformations undergone by coffee during roasting, the relationship between the heating mode and the material properties of coffee on the one hand and the non-stationary temperature profile within the bean on the other, are still far from being fully understood. In this presented work, a dynamic model is proposed for predicting the non-stationary thermal profile of coffee during roasting. The model is based on the assumption that the thermal effects occurring within the bean during roasting, such as moisture evaporation, can be approximately encompassed within a lumped together specific heat parameter. Using this hypothesis, it is possible to develop a mathematical model, which is quite simple in structure but still able to describe the two most important technological aspects, i.e. the evolution over time of the beans' average temperature and internal thermal gradient.

Key words:
Coffee roasting, dynamic model, lumped specific heat, temperature prediction, temperature distribution

Introduction

Roasting is a typical process in the food industry and is practiced in order to enhance the aromatic properties of the product. Heating power is supplied in such a way as to induce the removal of most humidity and partial or complete thermal decomposition of specific compounds of raw or green beans, which come from primary processing. Chemical changes induced in coffee by heating, most of which happen in the glucydic fraction[1] are accompanied by physical changes, indicating all those phenomena that do not concern molecular transformation:

– Loss of humidity,
– Dry mass loss,
– Volume increase,
– Drop in the luminosity and
– Colour shift.

The original greenish colour of raw coffee, ranging from a yellow to a blue sub-tone, depending on the variety of coffee and whether it underwent a wet or dry process, turns progressively to more or less dark brown, depending on the roasting degree.

It is possible to classify roasting methods into three groups:[2]

– Direct flame roasting: this is the most ancient way of roasting coffee. It consists in enveloping the container holding the coffee with a flame. Thermal transmission occurs through radiation between flames and the outside container's wall and through conduction between the inner container's wall and the bed of coffee beans, as well as from bean to bean;

– Preheated air roasting: this is the most commonly used method nowadays and consists of preheating an air-flow with a burner that is directed to a drum containing the loaded coffee. Heat transfer occurs through laminar flow convection between the air and coffee and through conduction between the beans;

– Fluidized bed roasting: consists of letting the preheated air pass through the bed of beans at high enough velocity to suspend it and give it a fluid-like appearance. Heat transfer occurs through turbulent flow convection.

*Corresponding author: Email: ireneo.kikic@dicamp.units.it;
Phone: +39 040 5583433; Fax: +39 040 569823

Drum processes usually require a longer roasting time ($t = 8\sim20$ min) and a higher inlet temperature of the roasting medium ($\theta = 400\sim500$ °C). Hence, these processes are often labeled HTLT (high temperature long time), even though higher air to coffee ratios allow a reduction in the inlet temperature of air. Thanks to better contact between the suspended beans, which are vigorously mixed, and the air, fluidization roasting allows lower temperatures ($\theta = 240\sim270$ °C) and shorter roasting times (~5 min). Another kind of roasting, somewhere in between the above described, is the spouted bed roasting. It exploits a particular kind a fluidization regime whereby the beans, although they are not suspended in the roasting medium, still undergo a good mixing and a relatively good delivery of heat. The roasting medium, both in the cases of drum and fluidized bed roasting, is not necessarily air, but may, most frequently, be a combustion gas coming from a burner. In this case the flame is located within the process line, while with air as a roasting medium the flame heats up the pipes externally, through which the air flows, with a less direct and hence less effective transmission of heat. Roasting processes can be further split between continuous and batch processes.

Parameters that influence its evolution, such as density, rheological features, volume and shape (and hence the specific surface), porosity of the beans, and transport properties, change dramatically[3] during roasting. Even the temperature is not constant in many processes but is adjusted for control purposes. The main goal of roasting is to induce a heating evolution within the bean matrix in such a way that the coffee's aroma may be fully developed and the beans homogenously cooked. The thermal history also influences other technologically important parameters, such as the puffing of beans, which is connected with their porosity and hence with the easiness of grinding and extraction. This stresses the importance of having a tool, which enables the prediction of coffee's response to different thermal treatments. This paper describes the development of a model regarding the heating of coffee during roasting, together with those experiments and comparisons with literature data, carried out to confirm the model's predictions. Some interesting work has been published recently on the same subject by Heyd *et al.*[4] and Hernandez *et al.*,[5] who used a model developed by Schwartzenberg.[6] The first model consists of a system of two differential equations, obtained from energy balance and from the material balance of moisture, and used the diffusivity of moisture as an adjustable parameter for fitting the experimental data. The second one gives predictions for the average temperature of coffee, neglecting the aspect of the internal distribution of temperature. The experimental data produced by these authors were used in the presented work for validating the model exposed in this paper.

Mathematical model

Initial assumptions:

– The grains are mixed and have the same temperature profile

– The roasting medium is mixed within the roaster

– The contact area between the coffee beans and the metal parts of the roaster is negligible

– The heat transfer coefficient between the roasting medium and the beans also takes into account the heat transfer from bean to bean

Fig. 1 synthesizes heat fluxes occurring during coffee roasting. The roasting medium enters at a mass flow rate $q_{m,gas}$ at a temperature T_{in}. After giving up part of its enthalpy to the coffee and to the thermal sinks, e.g. the heat dispersed into the outside environment through the walls, it leaves the roaster with a temperature T_{out}. The outlet gaseous mass flow rate is increased by the contribution of humidity and, to a lesser extent, volatiles released by the coffee.
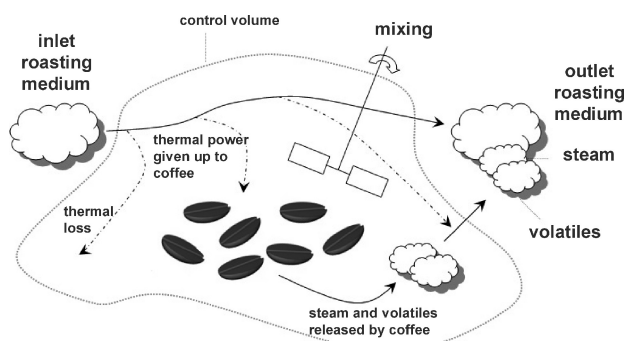

F i g . 1 – *Heat and mass fluxes during coffee roasting*

The thermal balance can be written as:

$$q_{m,gas}c_{p,gas}(T_{in})T_{in} - q_{m,gas}c_{p,gas}(T_{out})T_{out} + \ldots$$

$$- q_{m,vap}c_{p,vap}(T_{out})T_{out} - q_{m,vol}c_{p,vol}(T_{out})T_{out} = \quad (1)$$

$$= \{heat\ loss\} + \ldots + \{heat\ accumulation\}$$

Part of the accumulated heat contributes to raising the temperature of the beans' matrix (sensible heat) and part feeds endothermic phenomena (evaporation of humidity and endothermic effects, e.g. reactions of formation of phenolic and heterocyclic compounds).[3] Exothermic phenomena, e.g. pyrolysis of carbohydrates are present as well, and give away heat to the coffee.[7]

Hence:

$$\{heat \ accumulation\} = c_{p,dry} m_{dry} \frac{dT}{dt} +$$

$$+ c_{p,wat} m_{wat} \frac{dT}{dt} - \frac{dm_{dry}}{dt} \Delta h_{react} - \frac{dm_{wat}}{dt} \Delta h_{evap}. \tag{2}$$

The thermal balance of the roasting device can be broken down into two separate balances, of the coffee and of the roasting medium, respectively.

The thermal balance of coffee can be written as:

$$\Phi_{coffee} - q_{m,vap} c_{p,vap}(T)T - q_{vol} c_{p,vol}(T)T =$$

$$= c_{p,dry} m_{dry} \frac{dT}{dt} + c_{p,wat} m_{wat} \frac{dT}{dt} + \ldots \tag{3}$$

$$\ldots - \frac{dm_{dry}}{dt} \Delta h_{reactions} - \frac{dm_{wat}}{dt} \Delta h_{evap}$$

The thermal balance of the roasting medium can be written as:

$$q_{m,gas} c_{p,gas}(T_{in})T_{in} - q_{m,gas} c_{p,gas}(T_{out})T_{out} +$$

$$+ q_{m,vol} c_{p,vol}(T)T + \ldots + q_{m,vap} c_{p,vap}(T)T -$$

$$- q_{m,vap} c_{p,vap}(T_{out})T_{out} - q_{m,vol} c_{p,vol}(T_{out})T_{out} - \tag{4}$$

$$- \Phi_{coffee} = \{heat \ loss\}$$

Heat given away by the roasting medium to the coffee can be written as the product of an external heat transfer coefficient, the superficial area of the beans, and the difference in temperature between the roasting medium and the surface of the coffee (at temperature T_s):

$$\Phi_{coffee} = h A(T_a - T_s) \tag{5}$$

Since the reactor in which roasting occurs is stirred, the temperature of the roasting medium within the reactor T_a can be assumed as equal to the temperature of the roasting medium in the outlet stream:

$$T_a = T_{out}. \tag{6}$$

Eggers and Pietsch[3] plotted the loss of mass during roasting as a function of the temperature reached by the coffee, within the range 150–250 °C, reporting the results from different scholars, who used different roasting technnd coffee types.

All these data approximately align with a curve with expression:

$$\frac{\Delta m}{m_0} \approx 1.7880 \cdot 10^{-3} \exp(1.944 \cdot 10^{-2} \theta), \tag{7}$$

which implies that the evolution of coffee mass during roasting is approximately only a function of the initial mass and temperature. It is reasonable to hypothesize that this observation may extend to the two components of the coffee's overall mass: moisture and dry mass.

Using this hypothesis the time derivative of humidity and dry mass can be rewritten as:

$$\frac{dm_{wat}}{dt} = \frac{dm_{wat}}{dT}\frac{dT}{dt} \quad \text{and} \quad \frac{dm_{dry}}{dt} = \frac{dm_{dry}}{dT}\frac{dT}{dt}. \tag{8}$$

And eq. (3) can also be rewritten as:

$$m_{tot}\frac{dT}{dt}\left(c_{p,dry}\frac{m_{dry}(T)}{m_{tot}(T)} - \frac{1}{m_{tot}(T)}\frac{dm_{dry}}{dT}\Delta h_{react}(T) + \right.$$

$$+ c_{p,wat}\frac{m_{wat}(T)}{m_{tot}(T)} + \ldots \right)\left(\ldots - \frac{1}{m_{tot}(T)}\frac{dm_{wat}}{dT}\Delta h_{evap} - \right.$$

$$\left. - \frac{1}{m_{tot}(T)}\frac{dm_{dry}}{dT}c_{p,vol}T - \frac{1}{m_{tot}(T)}\frac{dm_{wat}}{dT}c_{p,vap}T \right) = \tag{9}$$

$$= h A(T_{out} - T_s)$$

or more compactly as:

$$m_{tot} c_{p,w} \frac{dT}{dt} = h A(T_a - T_s), \tag{10}$$

in which $c_{p,w}$, dimensionally a specific heat capacity, is a function of coffee's temperature and initial humidity, and is assumed to encompass the thermal effects occurring in coffee during roasting. The thermal flow from the roasting medium to the coffee causes the formation of a time-dependent thermal gradient within the beans. This aspect is crucial because it correlates with the homogeneity of the cooking.

The heat transfer within the beans' matrix can be described by equation:

$$c_{p,w}\rho \frac{\partial T_P}{\partial t} = \nabla \cdot (k \nabla T_P). \tag{11}$$

with initial and boundary conditions, respectively:

$$T_P = 0 \forall P, \quad k \nabla T_P \big|_s = h(T_{out} - T_s). \tag{12a, b}$$

It is common practice to idealize the shapes of those particles characterized by rounded outlines applying to the so-called equivalent sphere, which can be defined as the sphere having the same volume of the considered irregular particles (Kuni and Levenspiel[8]) This is also typically done with coffee (e.g. Eggers and Pietsch,[3] Heyd et al.,[4] Hernandez et al.,[5] Schwartzenberg,[6] Peker et al.[9]). Hence, to a first approximation, the complex geometry of the bean was replaced with the equivalent sphere, turning eq. (12) into the following:

$$c_{p,w}\rho \frac{\partial T(r)}{\partial t} = k\frac{1}{r^2}\frac{\partial}{\partial r}r^2\frac{\partial T(r)}{\partial r}, \qquad (13)$$

with initial and boundary conditions respectively:

$$T(r)=0, \; \forall r \in [0,R] \text{ and}$$
$$k\frac{\partial T(r)}{\partial r}\bigg|_{r=R} = h\cdot(T_{out}-T(R)). \qquad (14a, b)$$

The assumption is made that the combined internal and external heat transfer processes are described by a linear driving force approximation, which is based on a parabolic thermal profile within the bean,[10]

$$T(r) \approx T_1 + T_2 \cdot r^2, \qquad (15)$$

where T_1 and T_2 are functions of time.

The average temperature within the equivalent sphere is defined by:

$$T = \frac{3}{4\pi R^3}\cdot \int_0^R T(r)\,4\pi\,r^2\mathrm{d}r, \qquad (16)$$

Inserting eq. (15) into eq. (16) and integrating them gives:

$$T = \frac{3}{4\pi R^3}\cdot \int_0^R T(r)\,4\pi\,r^2\mathrm{d}r = T_1 + \frac{3}{5}T_2\cdot R^2. \quad (17)$$

From eq. (15):

$$\frac{\partial T(r)}{\partial r} = 2T_2 r, \qquad (18)$$

and the temperature on the bean's surface is:

$$T(R)=T_S = T_1 + T_2 \cdot R^2. \qquad (19)$$

Substituting $\partial T/\partial r$ and $T(R)$ (eqs. (18) and (19)) into the boundary condition (eq. (14b)) and expressing T_{out}, yields:

$$T_{out}=T_a = T_1 + T_2 R^2\left(1+\frac{2}{Bi}\right), \qquad (20)$$

where the Biot number Bi is expressed in terms of effective intraparticle thermal conductivity k:

$$Bi = \frac{h\cdot R}{k}. \qquad (21)$$

Isolating T_1 in eq. (17) and (20) and making them equal, gives:

$$T_2 = \frac{T_a-T}{R^2\left(\dfrac{2}{5}+\dfrac{2}{Bi}\right)}. \qquad (22)$$

Inserting eq. (18) into eq. (13) and derivation with respect to r gives:

$$c_{p,w}\rho \frac{\partial T}{\partial t} = 6kT_2 \qquad (23)$$

Combining eqs. (22) and (23) to eliminate T_2 yields a differential heat-balance equation with the linear driving-force expression:

$$c_{o,w}\rho \frac{\partial T}{\partial t} = U\cdot\frac{3}{R}\cdot(T_a-T) = U\cdot\frac{A}{V}\cdot(T_a-T), \quad (24)$$

where:

$$U = \frac{h}{\left(1+\dfrac{Bi}{5}\right)}. \qquad (25)$$

Combining eq. (17), (19) and (20), it is possible to obtain an expression for the ratio between average temperature over the whole bean's volume, and the surface temperature:

$$O_T = \frac{T}{T_s} = \frac{T_1+\dfrac{3}{5}R^2 T_2}{T_1+R^2 T_2} = \frac{\dfrac{T_1}{T_2}+\dfrac{3}{5}R^2}{\dfrac{T_1}{T_2}+R^2} =$$

$$= \frac{\dfrac{\left(\dfrac{2}{Bi}+1\right)T-\dfrac{3}{5}T_a}{T_a-T}+\dfrac{3}{5}}{\dfrac{\left(\dfrac{2}{Bi}+1\right)T-\dfrac{3}{5}T_a}{T_a-T}+1} = \frac{\left(\dfrac{1}{Bi}+\dfrac{1}{5}\right)T}{\left(\dfrac{1}{Bi}T+\dfrac{1}{5}T_a\right)}. \qquad (26)$$

This parameter can be monitored as a tool to prevent over-roasting of the surface and under-roasting of the core.

As the Bi number approaches 0, i.e. as the internal heat transfer is negligible compared to the external resistance, ratio O_T approaches unity, and the surface temperature equals the average temperature of the coffee bean:

$$\lim_{Bi\to 0} O_T = \frac{T}{T_S} \approx \frac{\left(\dfrac{1}{Bi}\right)T}{\left(\dfrac{1}{Bi}\right)T} = \frac{T}{T} \Rightarrow T_s=T_a. \quad (27)$$

As the Bi number tends to infinity, i.e. as the internal resistance is infinite and/or the external one is zero, the ratio O_T tends to T/T_a, and the external temperature tends to coincide with that one of the roasting medium:

T a b l e 1 – *Heat transfer parameters for various roasting processes*

Roaster type	U W m^{-2} K^{-1}	h W m^{-2} K^{-1}	k W m^{-1} K^{-1}	R mm	Biot –	IRHT %
drum roaster	2.84[12]	2.87 (eq. 24)	0.173[12]	3.5[3]	0.0058	1
spouted bed	14[11]	14.85 (eq. 24)	"	"	0.3004	6
fluidized bed	34.4÷ 72.9 (eq. 24)	40÷120[5]	"	"	0.8092 ÷ 2.4277	24 ÷33

$$\lim_{Bi \to 0} O_T = \frac{T}{T_S} \approx \frac{\left(0 + \frac{1}{5}\right)T}{\left(0 + \frac{1}{5}\right)T_a} = \frac{T}{T_a} \Rightarrow T_s = T_a. \quad (28)$$

In general, when $Bi \gg 5$, intraparticle thermal resistance dominates over the external heat-transfer resistance. In literature it is possible to find input data for eqs. (21), (25) and (26).

Thus, it is possible to estimate the Bi numbers for various processes and the relative importance of internal and external heat transfer. This is synthesized in Table 1 where reported values should be regarded as average values under typical operative conditions, while more rigorously, all these parameters are temperature dependent.

The relative importance of internal heat transfer was evaluated as:

% internal resistance to heat transfer

$$(\% \text{ IRHT}) = \frac{U \cdot R}{5k} \cdot 100. \quad (29)$$

As shown in Table 1, in the most important processes the Bi number is always inferior to 5, which means that the resistance to heat transfer always tends to be concentrated in the external film. In the case of drum roasting, and, to a lesser extent, in spouted bed roasting, internal resistance is completely negligible. In these kinds of processes, the thermal gradient is insignificant and can be neglected for modeling purposes. In the case of fluidized-bed roasting, the thermal gradient is more marked, with relatively higher surface temperatures. However, heat transfer coefficients are much higher, enabling a quicker heating rate compared to traditional roasters, all else being equal. The results obtained using this model, which will be addressed in the following as closed form model, are quite close to those achieved when modeling the beans' geometry in a much more realistic way and applying to the finite element method. This was verified in the present work by developing a model in which coffee was regarded as an engraved semi-hellipsoid with two axes of the same size and equal to half of the major axes and using the Galerkhin method in Femlab™ 3.1 to solve the time-dependent problem represented by eqs. (11) and (12a, b). Bean geometry was divided into very small finite-size tetrahedral elements through the automatic mesh generator of Femlab. The discretization error, that is the difference between the finite element representation and the real system, drops as the sizes of the elements decreases. At the same time the degrees of freedom, that is the number of the model's unknowns, increase with denser meshing.

As a compromise, a meshing was chosen that enabled a high quality of meshing, with a relatively small amount of elements. This was carried out by choosing the meshing represented in column C of Table 2. This Table shows that, compared to the chosen meshing, a ten-fold increase in the number of elements would produce just a 15 % increase in meshing quality, the latter being required as rule of thumb to be above 0.3 in order to achieve reliable results.[13]

The average size of the elements using the chosen meshing has an order of magnitude of 10^{-5} mL. Besides simulating at different roasting temperatures and at different external heat transfer coefficients, scenarios with different volumes and densities were also analyzed, since a remarkable change in physical properties occurs during roasting, and since this influences the heating. Simulations were split in two groups in regard to the roasting temperature and heat transfer coefficients, one referring to drum roasting and one to fluidized bed roasting. The parameters of the simulations are shown in Tables 3 and 4.

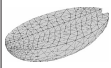T a b l e 2 – *Meshing options: the authors chose option C for solving the PDE problem*

	A	B	C	D
degrees of freedom	2897	4004	4915	39537
# of subdomain elements	1573	2322	2896	26982
# of boundary elements	782	854	992	3452
# of edge elements	188	165	172	269
minimum meshing quality	0.1312	0.2797	0.3239	0.3793

T a b l e 3 – *Parameters used in the simulations at drum roasting conditions*

|	ρ/kg m^{-3}	V/m^3	h/W m^{-2} K^{-1}	θ_a/°C
A	700	1.30974E-07	3.125	480
B	900	1.30974E-07	3.125	480
C	900	1.30974E-07	1.875	480
D	700	1.30974E-07	1.875	480
E	700	1.30974E-07	3.125	380
F	900	1.30974E-07	3.125	380
G	900	1.30974E-07	1.875	380
H	700	1.30974E-07	1.875	380
I	800	1.30974E-07	2.5	530
L	800	1.30974E-07	3.75	430
M	1000	1.30974E-07	2.5	430
N	800	1.30974E-07	2.5	330
O	800	1.30974E-07	1.25	430
P	600	1.30974E-07	2.5	430
Q	800	1.30974E-07	2.5	430
Q (+50)	800	1.93896E-07	2.5	430
Q (+100)	800	2.94919E-07	2.5	430
Q (+200)	800	3.87724E-07	2.5	430

T a b l e 4 – *Parameters used in the simulations at fluidized bed roasting*

	ρ/kg m^{-3}	V/m^3	h/W m^{-2} K^{-1}	θ_a /°C
A	600	1.30974E-07	100	220
B	1200	1.30974E-07	100	220
C	1200	1.30974E-07	15	220
D	600	1.30974E-07	15	220
E	600	1.30974E-07	100	200
F	1200	1.30974E-07	100	200
G	1200	1.30974E-07	15	200
H	600	1.30974E-07	15	200
I	900	1.30974E-07	50	240
L	900	1.30974E-07	50	180
M	900	1.30974E-07	50	220
M-50	900	6.54872E-08	50	220
M+100	900	2.94919E-07	50	220
N	900	1.30974E-07	50	200
N-50	900	6.54872E-08	50	200
N+100	900	2.94919E-07	50	200

The external heat transfer coefficients were arbitrarily chosen from the order of magnitude of values reported in Table 1, spouted bed being regarded as a fluidization regime and grouped as such.

Simulations were performed assuming an initial humidity of $w = 12$ %. Fig. 2 shows the evolution over time of the internal gradient, measured as $100 \cdot (T_{min} - T_{max})/T_{max}$, during a simulation of heating under drum roasting conditions. Fig. 3 shows an analogous simulation at fluidized bed roasting conditions. Comparing Figs. 2 and 3, it can be clearly seen that fluidized bed roasting is characterized by a much higher thermal gradient compared to drum roasting.
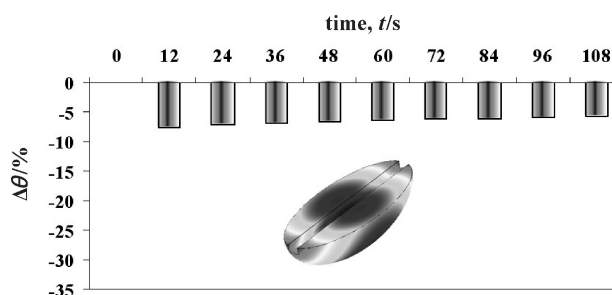
F i g . 2 – *Thermal gradient of a drum roasting simulation (Test Q: roasting temperature $\theta = 430$ °C, external heat transfer coefficient $h = 2.5$ W m^{-2} K^{-1})*
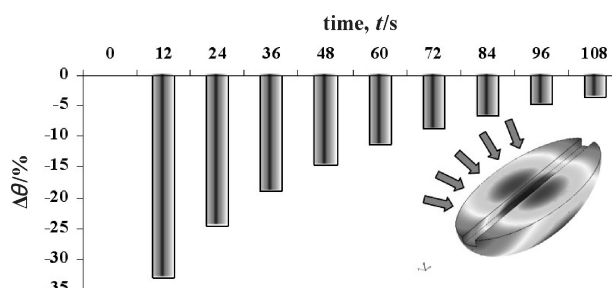
F i g . 3 – *Thermal gradient of a fluidized bed roasting simulation (Test M: roasting temperature $\theta = 220$ °C; external heat transfer coefficient $h = 50$ Wm^{-2} K^{-1})*

This gradient tends to level progressively but this occurs only as the average temperature gets close to its asymptote.

Figs. 2 and 3 also highlight the different temperature distributions on the surface of the bean in the two roasting modes and the tendency of heat to stagnate on the surface during fluidized bed roasting.

Table 5 shows the deviation between the closed form model and finite elements one, measured as the difference between the value of overall heat transfer coefficient calculated using eq. (25) and the one calculated from the finite element simulations fitting the data of average volumetric and surface temperature with the expression:

$$U = h\frac{(T_S - T_a)}{(T - T_a)}. \qquad (30)$$

Table 5 – *Different values of the external heat transfer coefficient obtained from eq. 25 and fitted with eq. 30 from simulations with the finite elements method*

	U_{calc}/W m^{-2} K^{-1}	U_{simul}/W m^{-2} K^{-1}	% error
fluidized bed			
A	80.348	79.673	0.85
B	80.348	82.78	−2.94
C	14.469	13.305	8.75
D	14.469	12.772	13.29
E	80.348	78.332	2.57
F	80.348	81.439	−1.34
A	80.348	79.673	0.85
H	14.469	11.882	21.77
I	44.552	38.724	15.05
L	44.552	37.315	19.393
M	44.552	40.455	10.126
M-50	45.55	37.596	21.157
M+100	43.371	38.531	12.561
N	44.552	38.298	16.33
N-50	45.55	37.479	21.537
N+100	43.371	38.672	12.15
drum			
A	3.101	3.022	2.63
B	3.101	3.022	2.63
C	1.866	1.785	4.57
D	1.866	1.785	4.57
E	3.101	3.022	2.63
F	3.101	3.022	2.63
G	1.866	1.785	4.57
H	1.866	1.785	4.57
I	2.485	2.399	3.6
L	3.716	3.654	1.69
M	2.485	2.399	3.6
N	2.485	2.399	3.6
O	1.246	1.18	5.57
P	2.485	2.399	3.6
Q	2.485	2.399	3.6
Q (+50)	2.483	2.399	3.51
Q (+100)	2.48	2.399	3.4
Q (+200)	2.478	2.399	3.32

Deviation is larger in fluidized bed roasting (average error 10.7 %, maximum error 21.8 %) compared to drum roasting, where external and overall heat transfer tend to merge (average error 3.6 %, maximum error 5.7 %).

Fig. 4 shows a comparison between the outputs of the two models when the deviation is the highest.
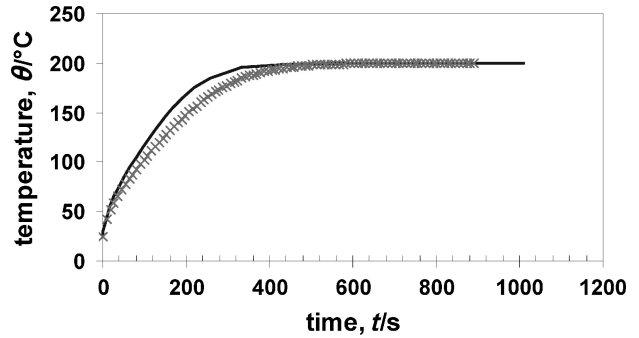

F i g . 4 – *Comparison between average temperature curves obtained from the closed form model (–) and from the finite element method (×) in the worst deviation scenario (fluidized bed – Test H: roasting temperature θ = 200 °C ; external heat transfer coefficient h = 15 W m^{-2} K^{-1})*

It is possible to get a better agreement between the two models by modifying eq. (25).

This can be written in dimensionless form as:

$$\frac{h}{U} = 1 + \frac{1}{5} Bi. \qquad (31)$$

It is possible to detect the presence of a second dimensionless number influencing heating by running a dimensional analysis for all variables involved in coffee heating.

Using the Buckingham method, the following product can be written:

$$\alpha^A k^B h^C U^D T_a^E \rho^F L^G, \qquad (32)$$

that yields, once the units are introduced:

$$\left(\frac{m^2}{s}\right)^A \left(\frac{m\,kg}{s^3 K}\right)^B \left(\frac{kg}{s^3 K}\right)^C \left(\frac{kg}{s^3 K}\right)^D K^E \left(\frac{kg}{m^3}\right)^F m^G, \qquad (33)$$

which corresponds to the following linear system:

$$\begin{cases} B + C + D + F = 0 \\ 2A + B - 3F + G = 0 \\ A + 3B + 3C + 3D = 0 \\ -B - C - D + E = 0 \end{cases} \qquad (34)$$

Solving the latter yields the following dimensionless numbers:

$$\frac{U}{h}, \quad \frac{h\,L}{k} = Bi, \quad \frac{a^3\,\rho}{h\,T_a\,L^3} = \frac{1}{Bi^3}\,\frac{h^2}{\rho^2 c_{p,w}^3\,T_a} \to \frac{U}{h},$$

$$Bi, \quad Y = \frac{h^2}{\rho^2 c_{p,w}^3\,T_a}. \tag{35}$$

The number denoted by letter Y represents a ratio between the heating power and the capability of coffee to adsorb it.

Eq. (30) was consequently replaced with the following empirical relationship:

$$\frac{h}{U} = 1 + a \cdot Bi^b Y^c. \tag{36}$$

Introduction of eq. (36) also modifies the connection between the average surface and the average volume temperature:

$$T_s = \frac{U}{h}T + T_a\left(1 - \frac{U}{h}\right) \to O_T = \frac{T}{T_s} = \frac{1 + a \cdot Bi^b Y^c}{1 + a\,\dfrac{T_a}{T}\,Bi^b Y^c}. \tag{37}$$

Using eq. (36) with the parameters in Table 6, which were obtained by fitting eq. (36) to the values of U calculated through eq. (30) from finite elements' simulations data, it is possible to evaluate U with an average error of around 0.5 %, and with a maximum error of 9 % (data in Table 7), thus making the outputs of the closed form and finite element models almost interchangeable, as shown in Fig. 5, where the outputs of the models are again compared in the worst agreement scenario. The degree of overlapping between the curves can be considered satisfactory.

T a b l e 6 – *Parameters of eqs. 36 and 37*

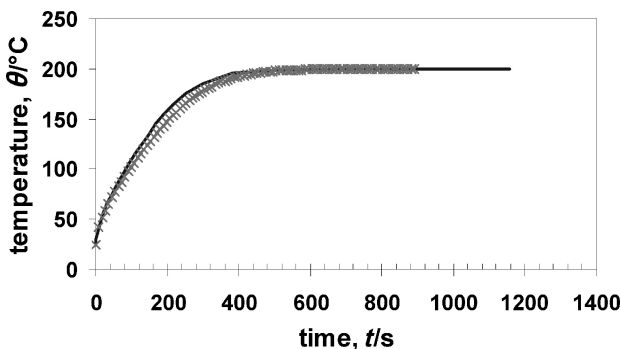| a	b	c
52.41	0.202	0.10746

F i g . 5 – *Comparison between average temperature curves form the closed form model (–) and from the finite element method (×) in the worst agreement scenario (fluidized bed – Test H: roasting temperature θ = 200 °C ; external heat transfer coefficient h = 15 W m⁻² K⁻¹)*

T a b l e 7 – *Different values of the external heat transfer coefficient obtained from eq. 34 and fitted with eq. 30 from simulations with the finite elements method*

	U_{calc}	U_{simul}	% error
fluidized bed			
A	74.085	79.673	−7.01
B	76.842	82.78	−7.17
C	13.198	13.305	−0.81
D	12.948	12.772	1.38
E	74.34	78.332	−5.1
F	77.078	81.439	−5.36
G	13.219	13.017	1.55
H	12.971	11.882	9.17
I	40.179	38.724	3.76
L	40.507	37.315	8.56
M	40.32	40.455	−0.33
M-50	40.67	37.596	8.18
M+100	39.963	38.531	3.72
N	40.424	38.298	5.55
N-50	40.771	37.479	8.78
N+100	40.069	38.672	3.61
drum			
A	2.899	3.022	−4.06
B	2.91	3.022	−3.69
C	1.77	1.785	−0.87
D	1.764	1.785	−1.17
E	2.896	3.022	−4.17
F	2.907	3.022	−3.8
G	1.768	1.785	−0.95
H	1.762	1.785	−1.26
I	2.34	2.399	−2.46
L	3.465	3.654	−5.17
M	2.345	2.399	−2.26
N	2.335	2.399	−2.66
O	1.188	1.18	0.7
P	2.328	2.399	−2.96
Q	2.338	2.399	−2.55
Q (+50)	2.334	2.399	−2.72
Q (+100)	2.329	2.399	−2.91
Q (+200)	2.326	2.399	−3.03

Model verification

Roasting data were produced in the laboratories of the Department of Chemical, Environmental and Raw Material Engineering of the University of Trieste. Coffee, with specifications as reported in Table 8, was roasted at 4 different temperatures ($\theta =$ 160 °C, 180 °C, 200 °C and 220 °C), in a fan oven. 3 samples of app. 50 g were roasted at each roasting temperature, yielding average temperature curves. Temperature was measured using a thermally insulated thermocouple K with a sheath diameter of 1 mm, inserted inside the bean through a hole drilled in such a way as to fit the sheath perfectly (Fig. 6). The results are shown in Fig. 7. The model's curves were achieved using the properties of the raw bean. Data at $\theta =$ 160 °C, were used to perform a fitting in order to estimate the value of the external heat transfer coefficient. The oven was assumed to work like a shelf dryer, where the external heat transfer coefficient mostly depends on the entity of the air flow. Hence, it was hypothesized that the value of the external heat transfer coefficient remained approximately constant under the considered roasting temperatures. The fitted value of the external heat transfer coefficient of $h = 26.7$ $Wm^{-2}K^{-1}$ was used to produce prediction curves at $\theta =$ 180 °C, 200 °C and 220 °C.

Fig. 8 shows the evolution of temperature both at the core of the bean and at the surface at $\theta =$ 180 °C roasting temperature. The results seem to confirm the consistency of the modeling approach described in this paper. The relative impact of internal resistance was around 17 %. Figs. 9 and 10 compare the output of the model with data reported by Eggers *et al.*[14] and Schenker *et al.*[15] respectively, who produced temperature data from fluidized bed roasting. In this case, since correlations for predicting the external heat transfer coefficient are avail-

T a b l e 8 – *Specifications of coffee used in the experiments*

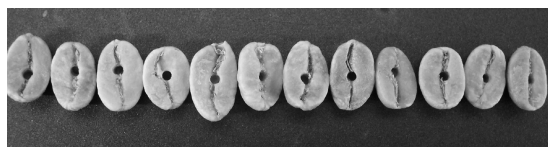| Property	Value
coffee	Washed India Arabica
humidity $w/\%$	9.1 ± 0.4
bean volume V/m^3 (liquid shift)	$1.69 \pm 0.08 \cdot 10^{-6}$
bean volume V/m^3 (semi-helipsoid)	$1.56 \pm 0.10 \cdot 10^{-7}$
bean mass m/g	0.163 ± 0.009

F i g . 6 – *Drilled coffee beans*
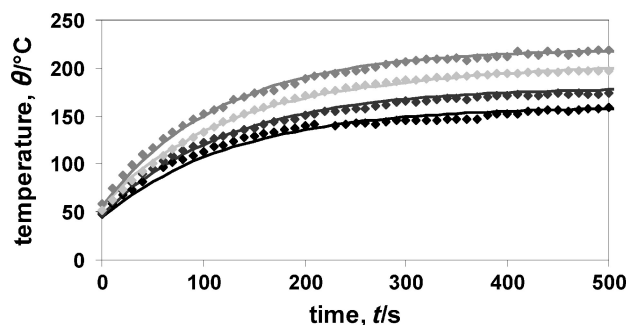
F i g . 7 – *Heating curves of coffee in the fan oven at $\theta =$ 160 °C (experimental data: ◆; model fit –), at $\theta =$ 180 °C (experimental data: ◆; model prediction –), at $\theta =$ 200 °C (experimental data: ◇; model prediction –), at $\theta =$ 220 °C (experimental data: ◆; model prediction –)*
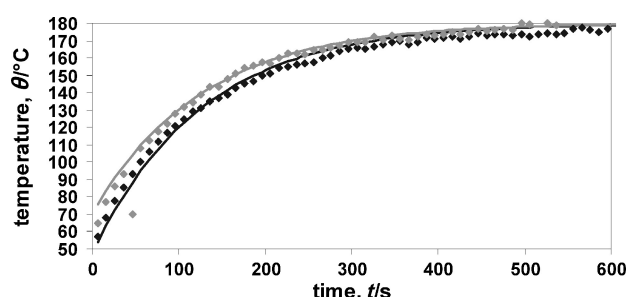

F i g . 8 – *Temperature evolution at the core (experimental data ◆; model prediction: –) and at the surface of the bean during roasting at $\theta =$ 180 °C (experimental data ◆; model prediction: –)*
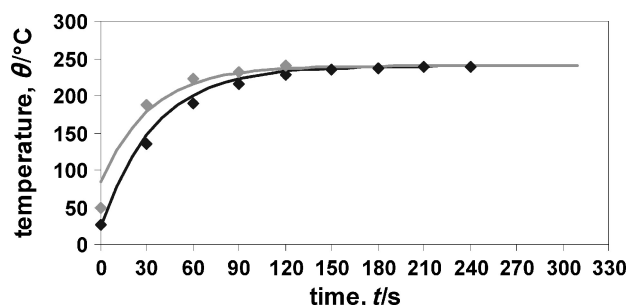

F i g . 9 – *Comparison of model predictions with fluidized bed roasting data by Eggers et al.:[14] core temperature (experimental data ◆; model prediction: –); surface temperature (experimental data ◆; model prediction: –)*

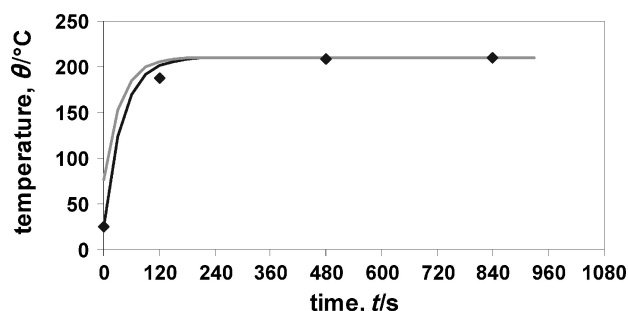
F i g . 1 0 – *Comparison of model predictions with fluidized bed roasting data by Schenker et al.:[15] core temperature (experimental data ◆; model prediction: –); surface temperature (model prediction: –)*

T a b l e 9 – *Average properties of arabica coffee[3]*

	humidity $w/\%$	bean mass m/g	bean density $\rho/g\ mL^{-1}$	bean volume V/mL
green coffee	10–12	0.15	1.2–1.4	0.11–0.13
medium roast	2–3	0.13	0.7–0.8	0.16–0.19

able (e.g. equation of Ranz[15]), the model can be used in a purely predictive way, i.e. without adjusted parameters. Authors have omitted to provide details of the coffee used. Hence the average parameters of Arabica coffees were taken as reference for geometry and initial humidity (Table 9), as given by Eggers and Pietsch.[3]

Figs. 11 and 12 compare model predictions with experimental data published by Heyd *et al.*[4] The amount of coffee ($m = 100$ g) used by these authors was large enough, compared to the mass flow rate of air ($q_m = 0.02$ kg s^{-1}), to induce a deviation from the set point value in the air temperature. This effect was to be taken into account because it influences the heating
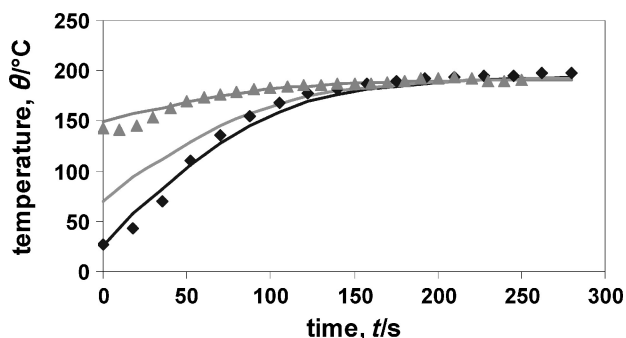

F i g . 1 3 – *Comparison of model predictions with roasting data by Hernandez et al.[5] (air temp. θ = 180 °C): core temperature (experimental data ◆; model prediction: –); surface temperature (experimental data ◆; model prediction: –)*

F i g . 1 4 – *Comparison of model predictions with roasting data by Hernandez et al.[5] (air temp. θ = 300 °C): core temperature (experimental data ◆; model prediction: —); surface temperature (experimental data ◆; model prediction: —)*
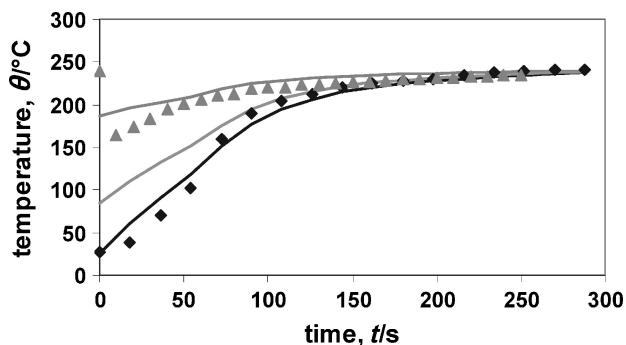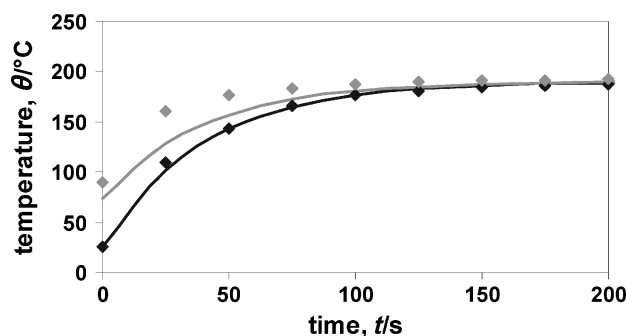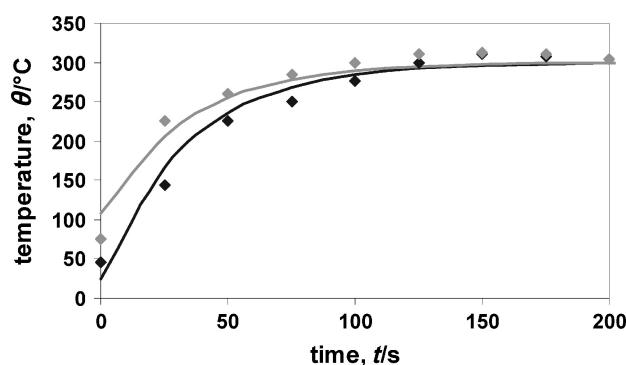

F i g . 1 1 – *Comparison of model predictions with spouted bed roasting data (air temp. θ = 190 °C) by Heyd et al.:[4] core temperature (experimental data ◆; model prediction: –); surface temperature (model prediction: –); outlet air temperature (experimental data ▲; model prediction: –)*

F i g . 1 2 – *Comparison of model predictions with spouted bed roasting data (air temp. θ = 240 °C) by Heyd et al.:[4] core temperature (experimental data ◆; model prediction: –); surface temperature (model prediction: –); outlet air temperature (experimental data ▲; model prediction: –)*

rate. Consequently, predictions were also performed for the outlet air temperature using eq. (4).

Figs. 13 and 14 compare forecasts from the model described in this study with data published by Hernandez *et al.*[5]

In this case, it was noticed that the model performed better at an air temperature of θ = 190 °C than it did at θ = 290 °C. This occurred because exothermic reactions occur at approximately θ = 250 °C, which lead the beans to burn and induce deviation from the otherwise roughly exponential heating kinetics. However, this is technologically irrelevant since the industrial roasting process is normally stopped well before this threshold. Concluding, these comparisons seem to confirm the viability of the suggested approach and the validity as a predictive tool of the model proposed by the authors.

Conclusion

In this study, a particle-based model of thermal transport occurring in coffee during roasting has been formulated and validated by comparison with experimental data. The model is based on heat trans-

fer theory and was developed with the main assumption that thermal effects occurring in coffee during roasting, such as evaporation of moisture, can be approximately encompassed within a lumped specific heat parameter. The model obtained was improved by exploiting data coming from simulations using the finite element method, on a semi-hellipsoidic shape closely resembling the real geometry of coffee, in order to correct an original simpler model based on the equivalent sphere. In spite of its simplicity, this model is able to provide relatively good predictions regarding the two technologically most important aspects of coffee heating:

– Evolution of the average temperature of coffee.

– Evolution of the thermal gradient within the beans.

This makes it a potentially valuable tool in industrial roasting, especially during the phase of tuning the process parameters. The model requires, as input data, the physical properties of green coffee, including the initial humidity, the temperature of the roasting medium and the external heat transfer coefficient. The main advantage of the model is the elementary character of its mathematical structure. Its main limitation resides in the downplay of some temperature-dependent properties and phenomena. However, model fits to the experimental data are good.

Nomenclature

A – external surface of coffee, m^2

Bi – Biot number, –

$c_{p,dry}$ – specific heat capacity of dry matter, $J\ kg^{-1}\ K^{-1}$

$c_{p,gas}$ – specific heat capacity of the roasting medium, $J\ kg^{-1}\ K^{-1}$

$c_{p,vap}$ – specific heat capacity of water vapor, $J\ kg^{-1}\ K^{-1}$

$c_{p,vol}$ – specific heat capacity of volatiles, $J\ kg^{-1}\ K^{-1}$

$c_{p,wat}$ – specific heat capacity of water, $J\ kg^{-1}\ K^{-1}$

h – external heat transfer coefficient, $W\ m^{-2}\ K^{-1}$

k – thermal conductivity, $W\ m^{-1}\ K^{-1}$

m_{dry} – coffee dry mass, kg

m_{wat} – coffee moisture mass, kg

m_0 – initial mass of coffee, kg

O_T – thermal homogeneity of coffee, –

P – generic point within the coffee bean, m; m; m

$q_{m,gas}$ – inlet mass flow rate of the roasting medium, $kg\ s^{-1}$

$q_{m,vap}$ – mass flow rate of water vapor released by the coffee, $kg\ s^{-1}$

$q_{m,vol}$ – mass flow rate of volatiles released by the coffee, $kg\ s^{-1}$

r – radial position in the equivalent sphere, m

R – radius of the equivalent sphere, m

U – overall heat transfer coefficient, $W\ m^{-2}\ K^{-1}$

$c_{p,w}$ – lumped heat capacity of coffee, $J\ kg^{-1}\ K^{-1}$

T – average temperature within the coffee bean, K

T_a – temperature of the roasting medium in the roaster, K

T_{in} – inlet temperature of the roasting medium, K

T_{max} – maximum temperature in the coffee bean, K

T_{min} – minimum temperature in the coffee bean, K

T_{out} – outlet temperature of the roasting medium, K

T_p – temperature in the point P, K

T_s – average surface temperature of the coffee bean, K

V – volume of coffee, m^3

w – mass fraction, %

Greek Symbols

Φ_{coffee} – heat flow rate to the coffee, W

Δh_{evap} – specific enthalpy of evaporation of moisture, $kJ\ kg^{-1}$

Δh_{react} – specific enthalpy of the reactions occurring in coffee, $kJ\ kg^{-1}$

Δm – roast loss, kg

ρ – density of coffee, $kg\ m^{-3}$

θ – temperature, °C

References

1. *Pittia, P., Dalla Rosa, M., Pinnavaia, G., Massini, R.*, Industrie Alimentari **35** (1996) 945.

2. Associazione del caffè di Trieste, Il libro del caffè, Tipografia Adriatica, Trieste, 1996.

3. *Eggers, R., Pietsch, A.*, Technology I: Roasting. In *Clarke R. J., Vitzhun O. J.* (Eds.), Coffee Recent Developments, Blackwell Science, Oxford, 2001, p. 91.

4. *Heyd, B., Broyart, B., Hernandez, J. A., Valdovinos-Tijerino, B., Trystram, G.*, Drying Technology **25** (2007) 1243.

5. *Hernandez, J. A., Heyd, B., Irles, C., Valdovinos, B., Trystram, G.*, Journal of Food Engineering **78** (2007) 1141.

6. *Schwarzenberg, H. G.,* Modelling bean heating during batch roasting of coffee beans, CRC Press LLC, 2002, p. 52.

7. *Strezov, V., Evans, T. J.,* International Journal of Food Properties **8** (2005) 101.

8. *Kunii, D., Levenspiel, O.,* Fluidization Engineering, Butterworth-Heinemann, New York 1990.

9. *Peker, H., Srinivasan, M. P., Smith, J. M., McCoy, B. J.*, AIChe Journal **38** (1992) 761.

10. *Škerget, M., Knez, Ž.*, Computers and Chemical Engineering **25** (2001) 879.

11. *Nagarju, V. D., Murthy, C. T., Ramalakshmi & Srinivasa Rao P. N.*, Journal of Food Engineering **31** (1997) 263.

12. *Sivetz, M., Desroisier, N. W.*, Coffee Technology, AVI, Westport, Connecticut, 1997.

13. *Comsol^{TM} Femlab 3.1, User Guide*

14. *Eggers, R., Blittersdorf, M., Fischer, C., Cammenga, H. K.*, Temperature Field during Roasting of Coffee Beans, Proceedings of the 20th ASIC Colloquium, 2004, p. 471–476.

15. *Schenker, S., Handschin, S., Frey, B., Perren, R., Escher, F.,* Structural properties of coffee as influenced by roasting conditions, Proceedings of the 8th ASIC Colloquium, 1999, p. 127–135.

16. *Bird, R. B., Stewart, W. E., Lightfoot E. N.*, Transport Phenomena, Wiley, 2001.